Autofocused, enhanced proton acceleration from a nanometer-scale bulged foil

H. Y. Wang,[1,2] X. Q. Yan,[1,2,3,a)] Y. R. Lu,[1] F. L. Zheng,[2] Z. Y. Guo,[1] W. J. Ma,[3,4] X. T. He,[2] T. Tajima,[4,5] D. Habs,[3,4] and J. E. Chen[1]
[1]*State Key Laboratory of Nuclear Physics and Technology, Peking University, Beijing 100871, China*
[2]*Center of Applied Physics and Technology, Peking University, Beijing 100871, China*
[3]*Max-Planck-Institut f. Quantenoptik, D-85748 Garching, Germany*
[4]*Fakultät f. Physik, LMU München, D-85748 Garching, Germany*
[5]*Photo-Medical Research Center, JAEA, Kyoto 619-0215, Japan*

(Received 2 June 2010; accepted 24 September 2010; published online 18 November 2010)

We report an autofocused, enhanced proton acceleration by the interaction of an intense laser pulse with a bulged target. These results are obtained from two-dimensional particle-in-cell simulations using a real Gaussian laser pulse, normally incident on a bulged/planar, 60 nm thick foil (C:H=1:1). When the laser pulse hits the precurved target, energetic protons are converged on the axis automatically. For the bulged foil, due to oblique incidence at the wing region, the efficient vacuum heating at larger incidence angles will result in more energetic hot electrons than from the flat foil. The enhancement of hot electron temperature and density will result in a larger longitudinal field, which contributes to an enhancement of proton energy. The maximum proton energy of 124 MeV is attained from a bulged target irradiated by a linear polarized laser pulse at an intensity of 1.3×10^{20} W/cm^2, which is two times higher than from the planar target (61 MeV). © *2010 American Institute of Physics*. [doi:10.1063/1.3503610]

I. INTRODUCTION

With the rapid advancement in laser technology, generation of energetic ion beam by interactions of an ultraintense laser pulse with a solid target is promising for many applications, such as proton radiography,[1] fast ignition for inertial confined fusion,[2–4] or hadron-therapy.[5] To date, mainly three laser-ion acceleration mechanisms have been demonstrated, i.e., the target-normal sheath acceleration (TNSA),[6–14] the break-out afterburner (BOA),[15,16] and the radiation pressure acceleration (RPA).[17–37] In target-normal sheath acceleration, the foil is thick enough (micrometer scale) so that the pulse cannot burn through the target, the ponderomotive force of the laser launches hot electrons from the front surface through the target. Upon reaching the back of the target, they establish a sheath electrostatic field which accelerates ions. When the target thickness is comparable to the skin depth, an enhanced TNSA, dubbed as BOA, shows that ions can be accelerated violently to GeV energies. In this case, the laser penetrates to the rear of the target and generates a large longitudinal electric field localized at the rear of the target, with the location of the peak field comoving with the ions. It is an effective combination of TNSA with the direct acceleration by the burning through a laser pulse. In the radiation pressure acceleration regime (RPA), the laser pulse is able to push the foil as a whole due to the fact that as it is reflected, it acts as a flying relativistic mirror.

The idea of ballistic focusing from a curved target shell to increase the ion density was proposed for thick targets several years ago.[38–40] Using a spherically shaped target, a focused proton beam is produced and used to heat a smaller volume to over 20 eV, which provides a unique method for creating isochorically heated high-energy density plasma states.[40] Based on the particle-in-cell (PIC) simulations, the generation of proton beams using a target with a concave back surface was first studied by Wilks *et al.*[38] They found that protons can be focused to a spot with high energy density. Comparing concave triangular, circular, and parabolic targets, Okada *et al.*[41] found that the parabolic target was most suitable for accelerating protons. Liu *et al.*[42] used parabolic targets and obtained a thin needle-profiled ion bunch. Via adding an axial filament stemming to the apex of a cone cavity (umbrella-like cavity target), Ma *et al.*[43] found that instead of diverging after the first focusing, as in the cone-shaped target, the protons produced from the umbrella-like target were well collimated.

In this paper, we report that hundred MeV protons can be generated from an ultrathin bulged foil irradiated by a real Gaussian laser pulse at an intensity of 1.3×10^{20} W/cm^2. An autofocused efficient proton beam is formed from the curved surface of the foil (see Fig. 1), which is similar to the results of thick foils. Since the pulse is in a Gaussian shape, the laser cannot penetrate the foil before the crest of the pulse comes; the ion acceleration follows the TNSA mechanism, as Fig. 1 shows. As the laser intensity gets close to its peak, the laser will penetrate the foil, then the enhanced TNSA regime begins, which has a higher electron temperature and higher longitudinal field as what Yin *et al.*[15,16] found. The simulation results indicate that linear polarized (LP) laser can accelerate protons up to 124 MeV from a bulged target, which is two times higher than that from the planar target (61 MeV) at the same laser intensity. The bulged target has a higher electron density and temperature than the planar target due to more efficient vacuum heating effects at the wing region,

a)Electronic mail: x.yan@pku.edu.cn.

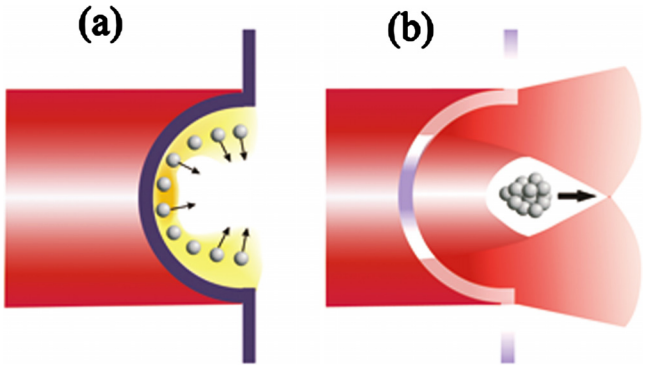

FIG. 1. (Color online) Schematic view of proton acceleration from a bulged target irradiated by a laser pulse. Here, the left light beam (red) represents the laser, the ball (gray) pellets are the protons, and the cloud (yellow) denotes electrons. (a) TNSA acceleration in the first stage. (b) Enhanced TNSA acceleration in the second stage.

which contributes to enhancement of the electrostatic field and proton energy for the bulged target.

II. SIMULATION PARAMETERS

In two-dimensional PIC simulations, the simulation box is $40\lambda \times 10\lambda$, where $\lambda = 0.8\ \mu$m is the laser wavelength, and contains 3200×800 cells. Each cell is filled with 100 quasiparticles. A LP laser pulse with a peak laser intensity of $I_L = 1.3 \times 10^{20}$ W/cm^{-2} is normally incident from the left side, the laser pulse is Gaussian both temporally and transversely, $I = I_L \exp[-(y/r_0)^2]\exp\{-[(t-t_L)/t_L]^2\}$, where $r_0 = 3\lambda$ and $t_L = 20$ T, T is the laser period. The corresponding peak dimensionless laser amplitude $a_0 = eE/(m_e\omega c)$ is 9.8, where E, ω, c, m_e, and e are the laser electric field, frequency, speed of light in the vacuum, electron mass, and charge, respectively. The initial temperature of electrons, protons, and carbon ions is 5 eV. The foil consists of a proton-carbon mixed plasma with an electron density $n_e = 80n_c$, where $n_c = \pi m_e c^2/(e\lambda)^2$ is the critical density, and the ratio of C:H=1:1. The plane foil with a thickness $d = 0.075\lambda$ is placed at $x = 3\lambda$. The bulged target with a convex radius $r = 3\lambda$ (see Fig. 1) has the same n_e and d as the planar target.

III. SIMULATION RESULTS

When the pulse hits the precurved bulged target, there is a perpendicular component of the electric field at the side of the target because of the oblique incidence of the pulse. It is well-known that the vacuum heating[44–46] depends on the incidence angle and the oblique incidence results in more efficient heating than the normal incidence. At the first stage, since the laser intensity is still low, the target is opaque, as what Figs. 1(a) and 2(a) show, and the foil cannot transmit the laser, and so, the protons are mainly accelerated by the sheath acceleration in TNSA regime. The deflection angle ϕ of the energetic protons can be determined in the nonrelativistic regime by[46] $\phi \approx \sqrt{\varepsilon_{\rm pk}/2m_pc^2}\sin\theta$, where θ is the incidence angle of the laser pulse, $\varepsilon_{\rm pk}$ is the proton kinetic energy, and m_p is the the proton mass. If we consider $\varepsilon_{\rm pk} = 100$ MeV, $\theta = 45°$, we can get $\phi \approx 9°$. It means the protons will propagate almost along the normal direction of the target and will be converged near the axis. Therefore, these energetic protons are automatically converged due to the geometric factor of the bulged target at the first stage of laser foil interactions.

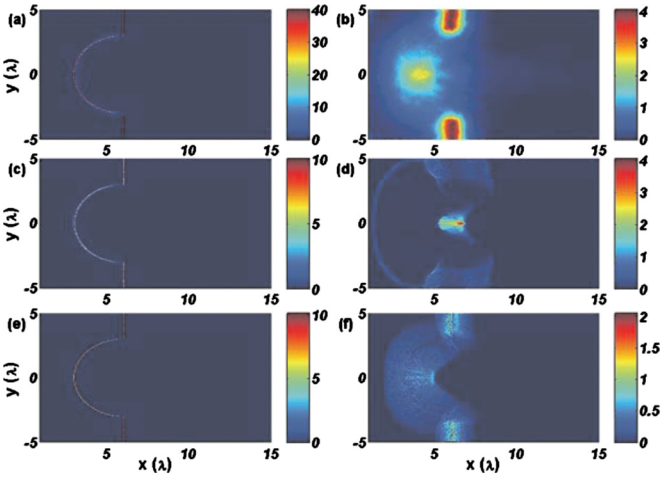

FIG. 2. (Color online) Foil density evolution (in units of critical density n_c) for LP laser at times [(a), (c), and (e)] $t = 6$ T and [(b), (d), and (f)] $t = 32$ T. The laser pulse is incident from the left and hits the plasma at $t = 2$ T (top: electrons, mid: protons, bottom: carbons).

As the laser intensity gets close to its peak, the laser penetrates the target (at $t = 16$ T), then the proton beam enters the enhanced TNSA regime [see Figs. 1(b) and 2(d)]. The autofocused proton beam can be clearly identified and an overdense proton bunch with 1λ diameter and 2λ length (about 10^9 protons) is observed in Fig. 2(d). Since the carbons are heavier than the protons, they cannot be focused like the protons, and they will expand as Fig. 2(f) shows.

The proton energy distributions E_y and E_x (normalized by $m_ec\omega/e$) for different targets at different time are shown in Figs. 3 and 4. At $t = 10$ T, the proton beam is in the TNSA regime with a low energy, as shown in Figs. 3(a) and 3(d), the laser cannot penetrate the target [see Figs. 3(b) and 3(e)] and the normalized longitudinal fields are about two for

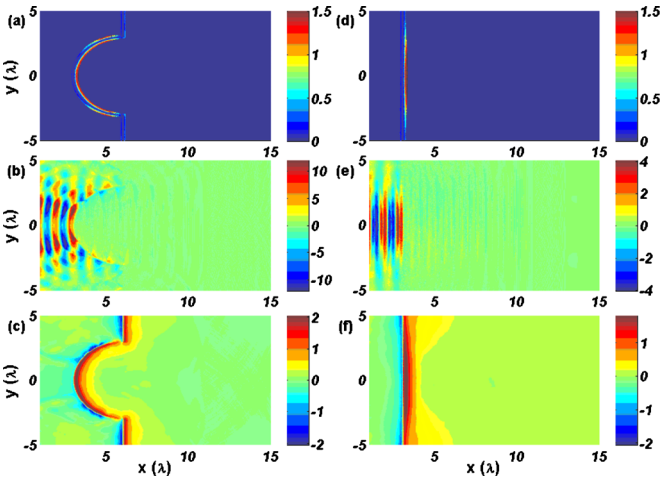

FIG. 3. (Color online) Proton energy (in units of MeV) and electric field (in units of $m_ec\omega/e$) for different targets with a LP laser at $t = 10$ T (TNSA regime). [(a) and (d)] Proton energy. [(b) and (e)] E_y. [(c) and (f)] E_x (left: bulged foil, right: planar foil).

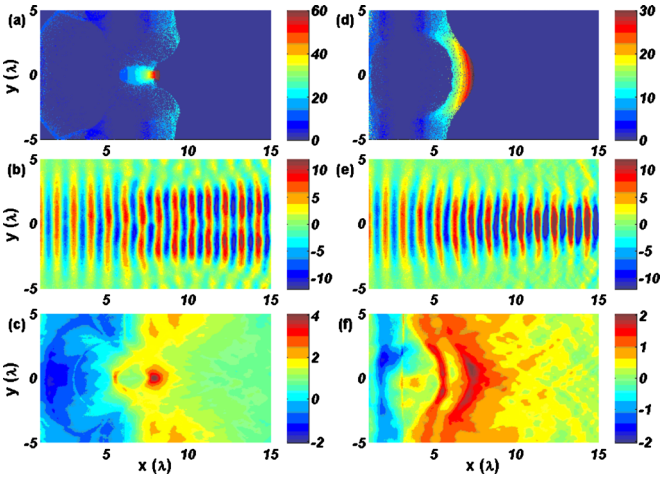

FIG. 4. (Color online) Proton energy (in units of MeV) and electric field (in units of $m_e c\omega/e$) for different targets with a LP laser at $t=36$ T (enhanced TNSA regime). [(a) and (d)] Proton energy. [(b) and (e)] E_y. [(c) and (f)] E_x (left: bulged foil, right: planar foil).

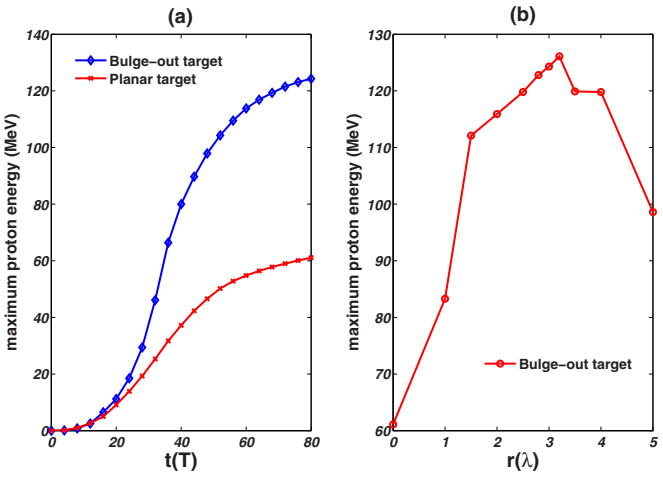

FIG. 6. (Color online) (a) Proton energy evolution for bulge-out target and planar target. (b) Maximum proton energy vs radius of bulged target for LP laser.

bulged target and one for planar target, as shown in Figs. 3(c) and 3(f). At $t=36$ T, the proton beam is accelerated in the enhanced TNSA stage, the laser burns through the target [see Figs. 4(b) and 4(e)] and generates more energetic hot electrons, which results in a higher longitudinal field, as shown in Figs. 4(c) and 4(f), with the location of the peak field comoving with the ions. The normalized longitudinal field is about four for bulged target and two for planar target, which are both higher than the longitudinal field in TNSA regime. The most energetic protons are located near the axis for the bulged target, while the protons are diverged in transverse direction in case of the planar foil, as shown in Figs. 4(a) and 4(d). Due to the efficient vacuum heating effect at the wing region, the hot electron temperature and the density will be higher for the bulged target, as shown in Fig. 5, which will result in a higher longitudinal field and higher proton energy. For the bulged target, the conversion efficiency from the laser pulse to the plasma is more than $\eta=24\%$, which is 1.7 times than that for the planar target ($\eta=14.1\%$). The higher efficiency and larger longitudinal field can explain the energy enhancement of the bulged target; accordingly, it makes hundred MeV protons possible at a modest laser intensity of 10^{20} W/cm^2. The higher conversion efficiencies would also be promising for the fast ignition of inertial confined fusion, where the efficiency should be at least larger than 10% to reduce the energy of the driver beam.[3]

Figure 6(a) shows the temporal evolution of the maximum proton energy with bulged and planar foils. It implies that the proton energy rises slowly before $t=14$ T in the TNSA regime, when the laser has not yet transmitted the foil. Between $t=14$ T and $t=50$ T, the foil becomes relativistic transparent, and the proton beam enters the enhanced TNSA regime, which results in a steep rise of the proton energy. After $t=50$ T, the laser pulse passes over the proton beam and the acceleration process terminates. The maximum proton energy for the bulged foil is up to 124 MeV, which is double of that from the planar foil (about 61 MeV). The proton energy spectrum for different targets at $t=80$ T is shown in Fig. 7. Figure 6(b) shows the dependence of the maximum proton energy on the radius of the bulged foil. It shows that the optimum radius is near $r=3\lambda$, which is nearly equal to the radius of the laser spot.

In order to understand the energy enhancement from the precurved thin target and to determine the optimum radius of the foil, it will be helpful to analyze the underlying heating mechanisms through PIC simulations. When an ultraintense LP laser irradiates a bulged target, both vacuum heating[47]

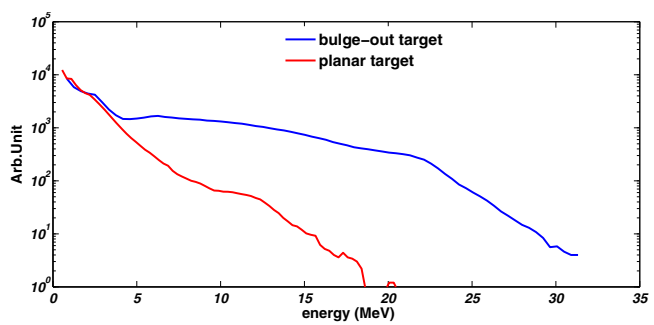

FIG. 5. (Color online) The electron energy spectrum for different targets with a LP laser at $t=80$ T.

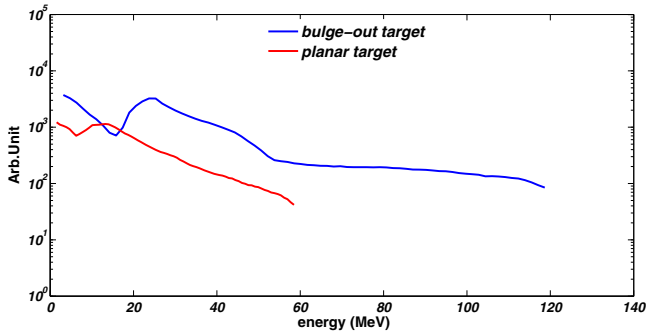

FIG. 7. (Color online) The proton energy spectrum for different targets with a LP laser at $t=80$ T.

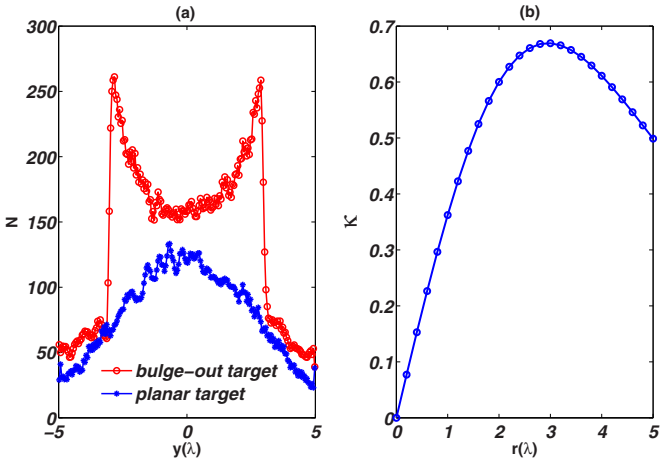

FIG. 8. (Color online) (a) Number of forward energetic electrons vs initial transverse positions in PIC simulations at time $t=20$ T. (b) Heating factor κ vs r.

and relativistic J×B heating[48,49] play an important role, while in case of the planar target, J×B heating is dominant and vacuum heating is less efficient under the normal incidence. The protons are directly accelerated by the charge separation field that is formed due to the electron departure from the target, so it is necessary to know the number of energetic electrons leaving the foil and their initial positions on the target. The number of energetic electrons leaving the target versus their initial transverse positions is plotted in Fig. 8(a), at the moment the crest of pulse comes to the foil. For the planar target, the transverse energetic electron distribution in the forward direction is Gaussian since the absorption efficiency of vacuum heating increases with the laser intensity.[48] Figure 8(b) shows the numbers of energetic electrons in the target center which are nearly the same for both targets, while there are two distinct peaks near $y=-3\lambda$ and $y=3\lambda$ in case of the bulged target. There the vacuum heating is highly efficient; accordingly, there will be more energetic electrons that depart from the target, which results in the larger electrostatic field compared to the flat target, as Figs. 3 and 4 show. In order to find the optimum radius at a given laser spot r_0, only vacuum heating effects are necessary to be considered because the field enhancement is mainly caused by this mechanism for the bulged target. A heating factor κ is introduced to evaluate laser absorption of the bulged target. If we take into account the incidence angle and the transverse profile of laser pulse, the heating factor for the unit arc length $rd\theta$ is proportional to the energy absorption dQ (Ref. 47),

$$d\kappa \propto dQ = P_L \times \eta_{\mathrm{vh}} \times rd\theta. \quad (1)$$

Here, P_L is the incoming laser power $P_L \propto c \times \exp[-(r \sin\theta/r_0)^2]\cos\theta/8\pi$, and η_{vh} is the absorption efficiency rate. In the ultrarelativistic limit, the absorption efficiency rate η_{vh} of vacuum heating is[47]

$$\eta_{\mathrm{vh}} = 4\pi\alpha/(\pi+\alpha)^2, \quad \alpha = \sin^2\theta/\cos\theta. \quad (2)$$

Here, θ is the incidence angle of the laser pulse. It peaks at $\alpha=\pi$ corresponding to $\theta_{\mathrm{opt}}=73.06°$. κ is determined by

$$\kappa = \int_0^{\pi/2} \exp[-(r \sin\theta/r_0)^2] \times \cos\theta \times \eta_{\mathrm{vh}} \times rd\theta. \quad (3)$$

Figure 8(b) shows the total heating factor κ peaks at $r=3\lambda$. As the maximum proton energy is enhanced with the heating factor increasing, then the optimum radius for maximum proton energy is $r/r_0=1$, which agrees well with simulation results in Fig. 4(b).

IV. CONCLUSION

In conclusion, autofocused proton acceleration from a bulged foil is proposed to enhance the ion energy. The maximum proton energy is over than a hundred MeV by using the bulged target at laser intensity of 1.3×10^{20} W/cm^2. It is two times higher than that from the flat target and the conversion efficiency from laser to plasma is as high as 24% that is promising for the hadron-therapy and the fast ignition of inertial confined fusion. In spite that such targets are challenging, however, the required laser intensity can be decreased by a factor of 4 if the maximum proton energy follows $I^{1/2}$ scaling at the relative lower laser intensity.[14,50] Accordingly, the bugled target can remarkably reduce the cost of a laser driven ion accelerator in the applications such as cancer therapy. Recently, these bulged diamond-like carbon foils have already been successfully fabricated at LMU/MPQ.[50] The next step is an experimental verification with a laser of a high pointing stability.

ACKNOWLEDGMENTS

This work is supported by NSFC under Grant Nos. 10935002 and 11025523. X.Q.Y. would like to thank the support from the Alexander von Humboldt Foundation. T.T. is supported in part by the Special Coordination Fund (SCF) for Promoting Science and Technology commissioned by the Ministry of Education, Culture, Sports, Science and Technology (MEXT) of Japan. D.H. is supported by Deutsche Forschungsgemeinschaft (DFG) through Transregio SFB TR18 and the DFG Cluster of Excellence Munich-Centre for Advanced Photonics (MAP).

[1] M. Borghesi, D. H. Campbell, A. Schiavi, M. G. Haines, O. Willi, A. J. MacKinnon, P. Patel, L. A. Gizzi, M. Galimberti, R. J. Clarke, F. Pegoraro, H. Ruhl, and S. Bulanov, Phys. Plasmas **9**, 2214 (2002).
[2] N. Naumova, T. Schlegel, V. T. Tikhonchuk, C. Labaune, I. V. Sokolov, and G. Mourou, Phys. Rev. Lett. **102**, 025002 (2009).
[3] M. Roth, T. E. Cowan, M. H. Key, S. P. Hatchett, C. Brown, W. Fountain, J. Johnson, D. M. Pennington, R. A. Snavely, S. C. Wilks, K. Yasuike, H. Ruhl, F. Pegoraro, S. V. Bulanov, E. M. Campbell, M. D. Perry, and H. Powell, Phys. Rev. Lett. **86**, 436 (2001).
[4] M. Temporal, J. J. Honrubia, and S. Atzeni, Phys. Plasmas **9**, 3098 (2002).
[5] S. V. Bulanov and V. S. Khoroshkov, Plasma Phys. Rep. **28**, 453 (2002).
[6] R. A. Snavely, M. H. Key, S. P. Hatchett, T. E. Cowan, M. Roth, T. W. Phillips, M. A. Stoyer, E. A. Henry, T. C. Sangster, M. S. Singh, S. C. Wilks, A. MacKinnon, A. Offenberger, D. M. Pennington, K. Yasuike, A. B. Langdon, B. F. Lasinski, J. Johnson, M. D. Perry, and E. M. Campbell, Phys. Rev. Lett. **85**, 2945 (2000).
[7] H. Schwoerer, S. Pfotenhauer, O. Jäckel, K.-U. Amthor, B. Liesfeld, W. Ziegler, R. Sauerbrey, K. W. D. Ledingham, and T. Esirkepov, Nature (London) **439**, 445 (2006).
[8] B. M. Hegelich, B. J. Albright, J. Cobble, K. Flippo, S. Letzring, M.

Paffett, H. Ruhl, J. Schreiber, R. K. Schulze, and J. C. Fernández, Nature (London) **439**, 441 (2006).
[9]A. J. Mackinnon, Y. Sentoku, P. K. Patel, D. W. Price, S. Hatchett, M. H. Key, C. Andersen, R. Snavely, and R. R. Freeman, Phys. Rev. Lett. **88**, 215006 (2002).
[10]S. P. Hatchett, C. G. Brown, T. E. Cowan, E. A. Henry, J. S. Johnson, M. H. Key, J. A. Koch, A. B. Langdon, B. F. Lasinski, R. W. Lee, A. J. Mackinnon, D. M. Pennington, M. D. Perry, T. W. Phillips, M. Roth, T. C. Sangster, M. S. Singh, R. A. Snavely, M. A. Stoyer, S. C. Wilks, and K. Yasuike, Phys. Plasmas **7**, 2076 (2000).
[11]L. Willingale, S. P. D. Mangles, P. M. Nilson, R. J. Clarke, A. E. Dangor, M. C. Kaluza, S. Karsch, K. L. Lancaster, W. B. Mori, Z. Najmudin, J. Schreiber, A. G. R. Thomas, M. S. Wei, and K. Krushelnick, Phys. Rev. Lett. **96**, 245002 (2006).
[12]L. Robson, P. T. Simpson, R. J. Clarke, K. W. D. Ledingham, F. Lindau, O. Lundh, T. McCanny, P. Mora, D. Neely, C. G. Wahlstrom, M. Zepf, and P. McKenna, Nat. Phys. **3**, 58 (2007).
[13]A. Yogo, H. Daido, S. V. Bulanov, K. Nemoto, Y. Oishi, T. Nayuki, T. Fujii, K. Ogura, S. Orimo, A. Sagisaka, J.-L. Ma, T. Zh. Esirkepov, M. Mori, M. Nishiuchi, A. S. Pirozhkov, S. Nakamura, A. Noda, H. Nagatomo, T. Kimura, and T. Tajima, Phys. Rev. E **77**, 016401 (2008).
[14]J. Fuchs, P. Antici, E. d'Humières, E. Lefebvre, M. Borghesi, E. Brambrink, C. A. Cecchetti, M. Kaluza, V. Malka, M. Manclossi, S. Meyroneinc, P. Mora, J. Schreiber, T. Toncian, H. Pépin, and P. Audebert, Nat. Phys. **2**, 48 (2006).
[15]L. Yin, B. J. Albright, B. M. Hegelich, and J. C. Fernández, Laser Part. Beams **24**, 291 (2006).
[16]L. Yin, L. Yin, B. J. Albright, B. M. Hegelich, K. J. Bowers, K. A. Flippo, T. J. T. Kwan, and J. C. Fernández, Phys. Plasmas **14**, 056706 (2007).
[17]A. Macchi, F. Cattani, T. V. Liseykina, and F. Cornolti, Phys. Rev. Lett. **94**, 165003 (2005).
[18]X. Zhang, B. Shen, X. Li, Z. Jin, F. Wang, and M. Wen, Phys. Plasmas **14**, 073101 (2007).
[19]S. S. Bulanov, A. Brantov, V. Yu. Bychenkov, V. Chvykov, G. Kalinchenko, T. Matsuoka, P. Rousseau, S. Reed, V. Yanovsky, K. Krushelnick, D. W. Litzenberg, and A. Maksimchuk, Med. Phys. **35**, 1770 (2008).
[20]X. Q. Yan, C. Lin, Z. M. Sheng, Z. Y. Guo, B. C. Liu, Y. R. Lu, J. X. Fang, and J. E. Chen, Phys. Rev. Lett. **100**, 135003 (2008).
[21]S. G. Rykovanov, J. Schreiber, J. Meyer-ter-Vehn, C. Bellei, A. Henig, H. C. Wu, and M. Geissler, New J. Phys. **10**, 113005 (2008).
[22]O. Klimo, J. Psikal, J. Limpouch, and V. T. Tikhonchuk, Phys. Rev. ST Accel. Beams **11**, 031301 (2008).
[23]A. P. L. Robinson, M. Zepf, S. Kar, R. G. Evans, and C. Bellei, New J. Phys. **10**, 013021 (2008).
[24]V. K. Tripathi, C. S. Liu, X. Shao, B. Eliasson, and R. Z. Sagdeev, Plasma Phys. Controlled Fusion **51**, 024014 (2009).
[25]L. L. Yu, H. Xu, W. M. Wang, Z. M. Sheng, B. F. Shen, W. Yu, and J. Zhang, New J. Phys. **12**, 045021 (2010).
[26]B. Eliasson, C. S. Liu, X. Shao, R. Z. Sagdeev, and P. K. Shukla, New J. Phys. **11**, 073006 (2009).
[27]M. Chen, A. Pukhov, T. P. Yu, and Z. M. Sheng, Phys. Rev. Lett. **103**, 024801 (2009).
[28]A. P. L. Robinson, P. Gibbon, M. Zepf, S. Kar, R. G. Evans, and C. Bellei, Plasma Phys. Controlled Fusion **51**, 024004 (2009).
[29]A. Macchi1, S. Veghini, and F. Pegoraro, Phys. Rev. Lett. **103**, 085003 (2009).
[30]Z. M. Zhang, X. T. He, Z. M. Sheng, and M. Y. Yu, Phys. Plasmas **17**, 043110 (2010).
[31]T. Esirkepov, M. Borghesi, S. V. Bulanov, G. Mourou, and T. Tajima, Phys. Rev. Lett. **92**, 175003 (2004).
[32]B. C. Liu, Z. H. He, X. Q. Yan, Z. M. Sheng, Z. Y. Guo, Y. R. Lu, and J. E. Chen, IEEE Transactions on Plasma Science **36**, 1854 (2008).
[33]A. Henig, D. Kiefer, K. Markey, D. C. Gautier, K. A. Flippo, S. Letzring, R. P. Johnson, T. Shimada, L. Yin, B. J. Albright, K. J. Bowers, J. C. Fernández, S. G. Rykovanov, H.-C. Wu, M. Zepf, D. Jung, V. Kh. Liechtenstein, J. Schreiber, D. Habs, and B. M. Hegelich, Phys. Rev. Lett. **103**, 045002 (2009).
[34]S. Steinke, A. Henig, M. Schnürer, T. Sokollik, P. V. Nickles, D. Jung, D. Kiefer, R. Hörlein, J. Schreiber, T. Tajima, X. Q. Yan, M. Hegelich, J. Meyer-ter-Vehn, W. Sandner, and D. Habs, Laser Part. Beams **28**, 215 (2010).
[35]B. Qiao, M. Zepf, M. Borghesi, and M. Geissler, Phys. Rev. Lett. **102**, 145002 (2009).
[36]X. Q. Yan, H. C. Wu, Z. M. Sheng, J. E. Chen, and J. M. Meyer-ter-Vehn, Phys. Rev. Lett. **103**, 135001 (2009).
[37]S. V. Bulanov, E. Y. Echkina, T. Z. Esirkepov, I. N. Inovenkov, M. Kando, F. Pegoraro, and G. Korn, Phys. Rev. Lett. **104**, 135003 (2010).
[38]S. C. Wilks, A. B. Langdon, T. E. Cowan, M. Roth, M. Singh, S. Hatchett, M. H. Key, D. Pennington, A. MacKinnon, and R. A. Snavely, Phys. Plasmas **8**, 542 (2001).
[39]H. Ruhl, S. V. Bulanov, T. E. Cowan, T. V. Liseikina, P. Nickles, F. Pegoraro, M. Roth, and W. Sandner, Plasma Phys. Rep. **27**, 363 (2001).
[40]P. K. Patel, A. J. Mackinnon, M. H. Key, T. E. Cowan, M. E. Foord, M. Allen, D. F. Price, H. Ruhl, P. T. Springer, and R. Stephens, Phys. Rev. Lett. **91**, 125004 (2003).
[41]T. Okada, A. A. Andreev, Y. Mikado, and K. Okubo, Phys. Rev. E **74**, 026401 (2006).
[42]M. P. Liu, H. C. Wu, B. S. Xie, J. Liu, H. Y. Wang, and M. Y. Yu, Phys. Plasmas **15**, 063104 (2008).
[43]Y. Y. Ma, Z. M. Sheng, Y. Q. Gu, M. Y. Yu, Y. Yin, F. Q. Shao, T. P. Yu, and W. W. Chang, Phys. Plasmas **16**, 034502 (2009).
[44]V. F. Dyachenko and V. S. Imshennik, Phys. Plasmas **5**, 413 (1979).
[45]F. Brunel, Phys. Rev. Lett. **59**, 52 (1987).
[46]T. Morita, T. Zh. Esirkepov, S. V. Bulanov, J. Koga, and M. Yamagiwa, Phys. Rev. Lett. **100**, 145001 (2008).
[47]P. Gibbon, *Short Pulse Laser Interactions with Matter* (Imperial College, London, 2005), Chap. 5, p. 160.
[48]W. L. Kruer and K. Estabrook, Phys. Fluids **28**, 430 (1985).
[49]P. Mulser, D. Bauer, and H. Ruhl, Phys. Rev. Lett. **101**, 225002 (2008).
[50]T. Tajima, D. Habs, and X. Q. Yan, Rev. Accel. Sci. Technol. **2**, 201 (2009).